Disproportionate impact of atmospheric heat events on lake surface water temperature increases

Wang, Xiwen; Shi, Kun; Qin, Boqiang; Zhang, Yunlin; Woolway, R. Iestyn

Nature Climate Change

DOI:
10.1038/s41558-024-02122-y

Published: 01/11/2024

Peer reviewed version

Editor summary:

'Lake surface water temperatures have increased over recent decades, mainly driven by atmospheric conditions. Here, the authors demonstrate that heat events drive a disproportionately large part of this lake surface warming and increases in lake heatwaves.

Peer Review Information:

Nature Climate Change thanks the anonymous reviewers for their contribution to the peer review of this work.

Figure or Table # Please group Extended Data items by type, in sequential order. Total number of items (Figs. + Tables) must not exceed 10.	Figure/Table title One sentence only	Filename Whole original file name including extension. i.e.: Smith_ED_Fig1.jpg	Figure/Table Legend If you are citing a reference for the first time in these legends, please include all new references in the main text Methods References section, and carry on the numbering from the main References section of the paper. If your paper does not have a Methods section, include all new references at the end of the main Reference list.
Extended Data Fig. 1	Characteristics and distribution of the 1260 studied lakes	fige1.jpg	**a-c** Histogram of the average depth (log10[m], **a**), surface area (log10[km^2], **b**), and elevation (m, **c**). **d** Spatial distribution of studied lakes.
Extended Data Fig. 2	Modelled vs. Lakes_cci LSWT	fige1.jpg	**a-b** Number of available Lakes_cci data from 2000 to

	during 2000–2020		2020 across all seasons (**a**) and in summer (**b**). Each range of the amount of validation data is presented on the x-axis, while the number of lakes falling into each category is depicted on the y-axis. **c-f** Correlation coefficients between FLake, CSFLake, and Lakes_cci throughout the year (**c**, **e**) and summer (**d**, **f**). **g-j** RMSEs (°C) between FLake, CSFLake, and Lakes_cci throughout the year (**g**, **i**) and summer (**h**, **j**). Note that there are four lakes not shown in FLake results (**c**, **d**) because they stayed frozen throughout the year.
Extended Data Fig. 3	Modelled vs. observed LSWT	fige3.jpg	**a** CSFLake vs. GloboLakes. **b** CSFLake vs. GLTC satellite data. **c** CSFLake vs. GLTC in-situ data. **d** CSFLake vs. in-situ data for seven Chinese lakes. The paired modelled and observed LSWT are daily means in **a** and **d**, and summer

			means in **b** and **c**. Each point represents the values of a paired CSFLake-observation data. The density of data is the normalized kernel density and is represented by the colour of points.
Extended Data Fig. 4	Validation of simulated LHW metrics from 2000 to 2020	fige4.jpg	**a-b** The mean absolute errors (MAEs) between LHW cumulative intensity calculated from Lakes_cci and modelled LSWT. **c-d** MAEs between LHW duration calculated from Lakes_cci and modelled LSWT. All the metrics were averaged over 2000–2020. In **b** and **d**, each point represents a lake; the density of data is the normalized kernel density and is represented by the colour of points.
Extended Data Fig. 5	The impact of HTEs on the intra-annual variability of LSWT	fige5.jpg	**a** Interannual variations of the intra-annual variability in CTL and CFT averaged over all studied lakes. The *p* values of trends were calculated using a two-tailed test. **b-c** Intra-annual

			variability trends (decade^{-1}) for each lake in CTL (**b**) and CFT (**c**).
Extended Data Fig. 6	Changes of LHW metrics from 1979 to 2022	fige6.jpg	**a-b** Annual trends in LHW duration (**a**; days decade^{-1}) and LHW cumulative intensity (**b**; °C days decade^{-1}). **c-d** Summer trends in LHW duration (**c**; days decade^{-1}) and LHW cumulative intensity (**d**; °C days decade^{-1}).
Extended Data Fig. 7	Relationships between air temperature, HTE metrics, and LHW metrics in summer	fige7.jpg	LHW duration trend vs. air temperature trend (**a**). LHW duration trend vs. HTE cumulative intensity trend (**b**). LHW duration trend vs. HTE duration trend (**c**). LHW cumulative intensity trend vs. air temperature trend (**d**). LHW cumulative intensity trend vs. HTE cumulative intensity trend (**e**). LHW cumulative intensity trend vs. HTE duration trend (**f**). Only lakes with non-zero trends in LHW metrics are shown in **a-f**. Mean LHW duration vs. mean air

			temperature (**g**). Mean LHW duration vs. mean HTE cumulative intensity (**h**). Mean LHW cumulative intensity vs. mean air temperature (**i**). Mean LHW cumulative intensity vs. mean HTE cumulative intensity (**j**). Pearson correlation coefficients (*r*) are shown in the upper corner.
Extended Data Fig. 8	HTEs contributions to trends in summer LHW metrics for all studied lakes	fige8.jpg	**a** Interannual variations of LHW duration (days) averaged across all studied lakes in CTL and CFT from 1979 to 2022. **b** Same as **a** but for LHW cumulative intensity (°C days). The *p* values were calculated using a two-tailed test.

10

Item	Present?	Filename Whole original file name including extension. i.e.: Smith_SI.pdf. The extension must be .pdf	A brief, numerical description of file contents. i.e.: *Supplementary Figures 1-4, Supplementary Discussion, and Supplementary Tables 1-4.*
Supplementary Information	Yes	SI.pdf	Supplementary Figure 1 and Supplementary Table 1.

11

Parent Figure or Table	Filename Whole original file name including extension. i.e.: *Smith_SourceData_Fig1.xls,* or *Smith_ Unmodified_Gels_Fig1.pdf*	Data description i.e.: Unprocessed western Blots and/or gels, Statistical Source Data, etc.
Source Data Fig. 1	fig1.csv	Statistical Source Data
Source Data Fig. 2	fig2.csv	Statistical Source Data
Source Data Fig. 3	fig3.csv	Statistical Source Data
Source Data Fig. 4	fig4.csv	Statistical Source Data
Source Data Extended Data Fig./Table 1	fige1.csv	Statistical Source Data
Source Data Extended Data Fig./Table 2	fige2.csv	Statistical Source Data
Source Data Extended Data Fig./Table 3	fige3.csv	Statistical Source Data
Source Data Extended Data Fig./Table 4	fige4.csv	Statistical Source Data
Source Data Extended Data Fig./Table 5	fige5.csv	Statistical Source Data
Source Data Extended Data Fig./Table 6	fige6.csv	Statistical Source Data
Source Data	fige7.csv	Statistical Source Data

Extended Data Fig./Table 7		
Source Data Extended Data Fig./Table 8	fige8.csv	Statistical Source Data

Disproportionate impact of atmospheric heat events on lake surface water temperature increases

Xiwen Wang [1, 2], Kun Shi [1, 3*], Boqiang Qin [1, 2], Yunlin Zhang [1, 3, 4], R. Iestyn Woolway [5]

[1] Key Laboratory of Lake and Watershed Science for Water Security, Nanjing Institute of Geography and Limnology, Chinese Academy of Sciences, Nanjing, China

[2] School of Geography & Ocean Science, Nanjing University, Nanjing, China

[3] University of Chinese Academy of Sciences, Beijing, China

[4] College of Nanjing, University of Chinese Academy of Sciences, Nanjing, China

[5] School of Ocean Sciences, Bangor University, Menai Bridge, Anglesey, UK

Xiwen Wang: wangxiwen_@outlook.com

Kun Shi: kshi@niglas.ac.cn

Boqiang Qin: qinbq@niglas.ac.cn

Yunlin Zhang: ylzhang@niglas.ac.cn

R. Iestyn Woolway: iestyn.woolway@bangor.ac.uk

*Corresponding author: Kun Shi, Nanjing Institute of Geography and Limnology, Chinese Academy of Sciences, 73 East Beijing Road, Nanjing 210008, P. R. China, Tel: + 86-25-86882174, Email: kshi@niglas.ac.cn

Abstract: Hot temperature extremes (HTEs) in the atmosphere can also affect lake surface water temperature (LSWT), but how this impact changes with global warming is not well understood. Here, we use numerical modelling and satellite observations to quantify the contribution of HTEs to variations in summer LSWT and lake heatwaves in 1260 waterbodies worldwide between 1979 and 2022. Over this time period, HTE duration and cumulative intensity over the studied lakes increased significantly, at average rates of 1.4 days decade^{-1} and 0.92 °C days decade^{-1}, respectively. Despite only accounting for 7% of the total summer days, HTEs are responsible for 24% of lake surface summer warming trends, with the most pronounced effect observed in Europe at 27%. Moreover, HTEs are key drivers of both the duration and cumulative intensity of lake heatwaves. Our findings underscore the pivotal role played by short-term climatic extreme events in shaping long-term LSWT dynamics.

Main text

Hot temperature extremes (HTEs) in the atmosphere have become increasingly frequent and severe on a global scale since 1950, a trend that persists across most regions irrespective of the indices used[1,2]. Between 1951 and 2003, HTEs occurred more frequently in over 70% of the land surface area, albeit with region-specific variability[3]. These variations arise from the partially independent drivers of HTEs and regional mean temperatures, leading to non-parallel long-term changes[4]. Warming of the annual highest near-surface air temperature over land is 45% higher than global mean surface temperature (sea surface temperature over the ice-free oceans and near-surface air temperature over land and sea ice)[2], a trend that has endured even during the so-called "warming hiatus"[5]. Evidence also points to an increase in the frequency of the most extreme heat events. In 2022, heatwaves swept across the globe, shattering records in Europe, China, the United States, Northern Africa, South America, and the Arctic[6]. Furthermore, the planet experienced its hottest June[7] and July[8] in 2023. The consequences of HTEs are already imposing severe and wide-ranging impacts on both natural[9] and social systems[10]. Between 1992 and 2013, anthropogenic extreme heat events resulted in trillions of economic losses, primarily due to infrastructure and crop damage[11].

Lakes worldwide store approximately 87% of Earth's usable liquid freshwater and provide crucial ecosystem services, including water supply, food production, transportation, recreation, tourism, and biodiversity protection[12-14]. Satellite data and in-situ measurements have unequivocally documented a warming trend in global lake surface water temperature (LSWT), at a rate of 0.34 °C decade^{-1} from 1985 to 2009[15,16]. The increase in LSWT can initiate a cascade of changes in lakes, both in terms of physical and biogeochemical processes[17]. Notably, this

includes the intensification of lake stratification[16], hindering the transport of oxygen from the surface to deeper waters, thereby inducing deoxygenation[18]. Subsequent hypoxic conditions at the lake bottom can promote the release of phosphorus from lake sediments[19]. Moreover, the discrete distribution of lakes limits the connectivity of native species to other habitats, and ecological disasters may occur when species fail to find refuge[20]. Compelling evidence underscores the far-reaching consequences of HTEs on lake ecosystems, manifesting as heightened LSWT, intensified deoxygenation in deeper layers[21], increased emissions of greenhouse gases[22], and the restructuring of fish communities[23].

Traditionally, research into LSWT responses to climate change has primarily centred on investigating how lakes respond to long-term climate warming signals[24]. These signals encompass a spectrum of climatic factors, including air temperature, solar radiation, wind patterns, and humidity, all of which contribute to variations in LSWT[16]. However, abrupt and intense fluctuations, exemplified by HTEs, have the potential to elicit dramatic and acute responses in lakes. Some studies have modelled or observed the impacts of the most severe atmospheric heatwaves on LSWT at regional and short-term scales, such as the 2018 European heatwave, which elevated LSWTs by 1.5–2.4 °C compared to the same period from 1981 to 2010[25], as suggested by model simulations during May–October in 2018. Satellite data showed that the record-breaking 2022 heatwave in China resulted in a 1.6 °C rise in lake skin temperature during June–August compared to 2000–2021[26]. However, the overarching contribution of contemporary HTEs to the long-term lake surface warming worldwide remains a critical knowledge gap. It is essential to recognize that while the direct effects of extreme events are transient, the cumulative impact of increasingly frequent events has the potential to

89 influence the statistical characteristics of LSWT at annual or longer time scales. Consequently,
90 there is an imperative need to quantitatively assess the role of present-day HTEs in driving lake
91 surface warming trends. Insights into the alterations of LSWT triggered by HTEs can
92 disentangle the complex interplay of individual processes underlying the thermal responses
93 observed in lake surfaces to changing atmospheric conditions.

94 Our investigation focuses on the impacts of HTEs on changes in the long-term trend of
95 LSWT and the emergence of lake heatwaves (LHWs), characterized by prolonged periods of
96 extremely hot LSWTs. Specifically, HTEs are defined as days with daily mean air temperature
97 above the 95th percentile of the 1979–2022 distribution[27]. LHW is defined as five or more
98 consecutive days where daily mean LSWT exceeds the 90th percentile of the 1979–2022
99 distribution[28]. This study focuses on HTEs during the summer period (1 July–30 September for
100 the Northern Hemisphere and 1 January–31 March for the Southern Hemisphere[15,29]). Daily
101 mean air temperature data from the European Centre for Medium-Range Weather Forecasts
102 Reanalysis v5-Land (ERA5-Land)[30] was used to detect HTEs. Our approach encompasses two
103 key steps: firstly, we selected 1260 lakes from around the world (Extended Data Fig. 1), ranging
104 between 0.2 and 400 m in average depth, between 0.6 and 16718 km^2 in surface area, and
105 between −216 and +5202 m in elevation. We used the Freshwater Lake (FLake) model[31] to
106 simulate LSWT, with a tuning procedure for three model parameters[32], including the light
107 extinction coefficient, ice albedo, and a multiplication factor to adjust the mean lake depth. The
108 tuning procedure minimizes model errors for each lake using satellite-derived LSWT as a
109 reference (see Methods). Hourly meteorological forcing for FLake was derived from ERA5-
110 Land. Specifically, air temperature, humidity, wind speed, surface pressure, and downward

shortwave/longwave radiation are required (see Methods). Modelled LSWT and LHWs have undergone validation (Extended Data Figs. 2, 3, and 4). Interannual changes in LSWT and LHWs from 1979 to 2022 were analysed using model simulations annually and during each summer. Subsequently, we used both statistical and numerical-experimental methods to explore the influence of HTEs on LSWT and LHWs during the summer period only. This is because annual statistics of LSWT and LHWs are not directly comparable among the studied lakes due to the variable duration of ice cover in each lake. Our key finding is that HTEs contribute 24% to the long-term trends in LSWT for all studied lakes, with a pronounced impact observed, particularly in the case of European lakes. Additionally, HTEs are found to intensify and prolong LHWs in European lakes.

Lake surface warming trends from 1979 to 2022

To provide a representative view of real-world lake conditions, we conducted a control experiment (CTL) to reconstruct LSWT from 1979 to 2022. The modelled LSWT averaged across all studied lakes exhibit a notable increase both annually (0.13 °C decade^{-1}) and during the summer months (0.23 °C decade^{-1}) (Fig. 1). The rate of change during summer is broadly consistent with findings from satellite data (0.20 ± 0.01[33] vs. 0.24 °C decade^{-1} during 1995–2022). The spatial patterns of summer mean LSWT change align with those reported from previous studies that investigated changes in LSWT, based on data from (i) the Global Lake Temperature Collaboration (GLTC)[15] and (ii) the Global Observatory of Lake Responses to Environmental Change (GloboLakes)[16]. These studies have collectively shown a pervasive warming trend globally, with European lakes experiencing the most rapid increase. Specifically,

the rate of change in summer mean LSWT for European lakes (located between 35–70°N and 10°W–50°E) in CTL is 0.42 °C decade^{-1}, approximately twice the average of all studied lakes. In regions such as North America, northern Europe, the Arctic, and certain areas of the Tibetan Plateau, the rate of change in summer mean LSWT surpasses that of the annual mean. These regions primarily consist of cold boreal lakes, which remain ice-covered until April–June. Conversely, in warm-climate regions, LSWT demonstrates comparable or even faster increases in other seasons relative to summer. These areas encompass lakes situated on the northern fringe of the Mediterranean, southern North America, and southeastern China. This intra-annual heterogeneity in lake surface warming has been previously identified in regional in-situ[34] and modelling studies[32]. There are exceptions to these trends, with certain regions in northern North America, northern East Asia, South Asia, southern South America, southern Africa, and central Australia displaying insignificant trends in annual and summer mean LSWT.

Contribution of HTEs to long-term lake surface warming

To characterize the interannual variation of HTEs, we computed two metrics: HTE duration (expressed in days) and cumulative intensity (calculated in °C days). Duration refers to the total number of days with HTEs during the summer months of each year. Cumulative intensity describes the severity of these extremes by calculating the average yearly deviation from the normal air temperature across all HTE events (see Methods). This deviation is calculated cumulatively for each uninterrupted block of HTEs, representing the overall heat stress. From 1979 to 2022, most lakes experience hotter and extended extreme summers (Fig. 2). Notably, all five of the hottest summers on record occurred within the 21st century, with the

summer of 2022 ranking as the hottest and most prolonged. The duration and cumulative intensity of HTEs averaged across all studied lakes in 2022 was 12.5 days and 12.9 °C days, respectively. HTE duration and cumulative intensity averaged over all studied lakes have exhibited statistically significant increases, at rates of 1.4 days decade^{-1} and 0.92 °C days decade^{-1}, respectively. This phenomenon of increasing HTEs is also evident at regional scales. In general, midlatitude lakes, particularly those in Europe, northern and eastern East Asia, western and eastern North America, and various parts of Africa and South America, are experiencing more extreme hot summers. These findings are consistent with observations, albeit assessing different metrics[2]. However, there are exceptions, with some regions in southern Africa, northern North America, Australia, and the Indian Peninsula displaying slight changes in both HTE metrics.

To investigate the relationships between HTE metrics (specifically, duration and cumulative intensity) and summer mean LSWT, linear regression models were used (Fig. 3). We detrended HTE duration and cumulative intensity (predictor variables), and summer mean LSWT (response variable) to construct linear regression models for each lake. The extent to which the variability in summer mean LSWT can be attributed to the variability in HTE metrics is captured by the explained variances of the linear regression models. The significance of the fitted coefficients offers insights into the importance of the two HTE metrics: if a coefficient derived for an HTE metric is statistically significant, it signifies a relationship between the metric and the variability of summer mean LSWT. In addition, we incorporated the raw HTE metrics, without removing any long-term trends, into the linear regression models and computed the trend of the response variable. The ratios of derived trends to summer mean

LSWT trends in CTL provide insights into the proportion of summer mean LSWT trends explained by the HTE metrics. HTE metrics explain approximately 39% of the variance in summer mean LSWT across all the studied lakes, with the largest explained variances found in high-latitude lakes in the Northern Hemisphere (Fig. 3a). Specifically, HTE duration is significantly associated with summer mean LSWT in most of the studied lakes (1069 out of 1260), with 99% of them having positive coefficients, implying that summer mean LSWT increases with the prolongation of HTEs. Conversely, HTE cumulative intensity appears to be a significant factor for 84 lakes. HTE metrics play a considerable role in explaining trends across a spectrum of lakes, including those with high explained variance ratios (such as eastern North America and northern Europe) as well as lakes with lower explained variance ratios (like eastern China and eastern South America) (Fig. 3b).

In addition to our linear regression analysis, we adopted a numerical-experimental approach to explicitly quantify the impact of HTEs on summer mean LSWT trends. In this experimental setup, referred to as the counterfactual experiment (CFT), we removed the influence of HTEs from the meteorological forcing. Specifically, if HTE occurs on one day, we scaled the 24-hour forcing data to ensure that the daily mean of each meteorological variable equals the mean value on that day from 1979 to 2022. Subsequently, we employed forcing data with the HTEs removed to drive the FLake model. The contribution of HTEs on summer mean LSWT trends for each lake can therefore be computed as

$$\frac{\mathrm{Trend}_{\mathrm{CTL}} - \mathrm{Trend}_{\mathrm{CFT}}}{\mathrm{Trend}_{\mathrm{CTL}}} \times 100\% \quad (1)$$

where $\mathrm{Trend}_{\mathrm{CTL}}$ and $\mathrm{Trend}_{\mathrm{CFT}}$ are trends in CTL and CFT, respectively. HTE contribution for a specific region is computed from LSWT averaged across all studied lakes of that region (see

199 Methods). Probability distributions of summer mean LSWT trends in each lake from CTL and
200 CFT are distinct ($p < 0.01$; Fig. 4a). CFT shows a lower change rate of 0.17 °C decade^{-1} for
201 summer mean LSWT averaged across all studied lakes compared to the CTL scenario (Fig 4b).
202 Therefore, HTEs contribute approximately 24% of the summer mean LSWT trend for all
203 studied lakes (27% for European lakes). The spatial distribution of contribution values, as
204 shown in Fig. 4c, is similar to patterns shown in Fig. 3b. Notably, lakes exhibiting contributions
205 larger than 20% can be found worldwide, particularly concentrated in Europe, eastern China,
206 North America, and eastern South America. It is noteworthy that the impact of HTEs on summer
207 mean LSWT is intensifying, as evidenced by the temporal variation in differences in summer
208 mean LSWT between the CTL and CFT scenarios (Fig. 4d), which is particularly pronounced
209 in Europe. Additionally, we observed that HTEs facilitate the change rate of intra-annual
210 variability, which is the coefficient of variation computed from the monthly mean LSWT, by
211 31% for all studied lakes, with the most apparent influence in Europe (Extended Data Fig. 5).
212 In summary, our study employs both statistical and numerical-experimental approaches to
213 assess the relationship between HTEs and summer mean LSWT. These two distinct
214 methodologies demonstrate that HTEs exert a noticeable influence on the summer warming of
215 lake surfaces, with European lakes emerging as particularly susceptible to these effects.
216
217 **Contribution of HTEs to LHW changes**
218 The enhanced long-term surface warming trends coincide with an increased probability of
219 lakes experiencing LHWs. We computed metrics for LHWs the same as HTEs, i.e., LHW
220 duration and cumulative intensity, but for each summer and year separately. From 1979 to 2022,

LHW duration increases at a rate of 1.9 days decade^{-1} in summer and 4.4 days decade^{-1} annually, with lakes in eastern and central America, Europe, and the Tibetan Plateau changing fastest (Extended Data Fig. 6a&c). LHW cumulative intensity also increases worldwide (3.37 °C days decade^{-1} in summer and 3.70 °C days decade^{-1} in annual), but European lakes increased the most (Extended Data Fig. 6b&d).

We investigated relationships between summer air temperature, HTE metrics, and summer LHW metrics (Extended Data Fig. 7). Trends in summer LHW duration and cumulative intensity both exhibit the strongest correlation with trends in summer air temperature (r = 0.20 and r = 0.30). This implies that the year-to-year variations in these two LHW metrics are both primarily influenced by trends in summer air temperature. Mean summer LHW cumulative intensity shows a strong positive correlation with mean HTE cumulative intensity (r = 0.63). Consequently, the primary factor influencing the spatial distributions of summer LHW cumulative intensity is HTE cumulative intensity.

In CFT, summer LHW duration and cumulative intensity exhibit statistically significant but slower rising trends compared to CTL (Extended Data Fig. 8). On average, for all studied lakes, summer LHW duration and cumulative intensity increase at rates of 1.2 days decade^{-1} and 1.71 °C days decade^{-1} in CFT, suggesting contributions of 35% and 49% from HTEs, respectively. This finding addresses the importance of HTEs in the prolongation and aggravation of LHWs.

Discussion

In this study, both statistical and numerical-experimental results support that HTEs

promote lake surface warming worldwide during the summers of 1979–2022, with hotspots seen in Europe, eastern China, Central America, and eastern South America. Among these, LSWT and LHWs in European lakes, which experience the most severe and prolonged extreme summers, are mostly affected. We disentangle the effects of HTEs on LSWT from the long-term climate warming signal and present new insights into global lake responses to climate change, as well as new evidence for climate change impacts on LSWT and LHWs. Considering the substantial impacts of HTEs on LHWs, more attention should also be given to the mechanism of temperature extremes propagation from the atmosphere to lakes. As FLake omits many processes affecting LSWT, for instance, horizontal circulations, cold inflows from glacial meltwater, fluctuations in water levels, etc., some lakes affected by these intrinsic deficiencies were not considered in this study to ensure the accuracy of modelled LSWT. We would expect that these unresolved processes may mitigate or aggravate the effects of HTEs on lakes, given their important roles in regulating LSWT. In addition, HTEs do not solely occur in summer but also during the colder months, as evidenced by winter warm spells reported in several regions[35,36]. These events may affect lake thermal structure and ecosystems by altering ice phenology, for instance, earlier ice break-up results in earlier lake surface heating[37] and an earlier growth season for phytoplankton[38].

Even with 1.5 °C of warming, HTEs are projected to increase and strengthen across all continents[2]. This escalation in extreme events is a natural consequence of the long-term climate warming trend driven predominantly by greenhouse gas emissions[2]. However, HTEs are also influenced by factors at regional or local scales[2], such as atmospheric dynamics (stronger heatwaves in Europe than other mid-latitude regions[39]), land-atmosphere feedbacks (“hotter

and drier" in tropical regions[40]), and land use (the role of urbanization in China's 2013 extreme summer heat[41]). Collectively, these factors contribute to the inherent spatial heterogeneity of HTEs[2], including the most severe events[42]. This highlights the imperative need for regions worldwide to prepare for the increasing occurrence of severe HTEs and their consequential impacts on LSWT and lake ecosystems. Given that changes in LSWT will also affect the vertical thermal structure of lakes, future research can focus on investigating the impact of HTEs in shaping the distribution of water temperature, such as stratification, using sophisticated process-based models. Our study underscores the critical need to enhance the performance of climate models in simulating climate extremes[43,44]. Such improvements are vital for accurately assessing the future impact of HTEs on lake ecosystems and, consequently, for informed climate mitigation and adaptation strategies.

Acknowledgements

This work was supported by the National Natural Science Foundation of China (U22A20561), the Tibetan Plateau Scientific Expedition and Research Program, (2019QZKK0202), the NIGLAS foundation (E1SL002), and the Water Resource Science and Technology Project in Jiangsu Province (2020057). RIW was supported by a UKRI Natural Environment Research Council (NERC) Independent Research Fellowship (grant number NE/T011246/1) and NERC grant reference number NE/X019071/1, "UK EO Climate Information Service".

Author contributions

X.W.W. conceived the work, performed the numerical modelling, completed the data

analysis, and wrote the manuscript. K.S. conceived the work and revised the manuscript. B.Q.Q., Y.L.Z., and R.I.W. revised the manuscript.

Competing interests

The authors declare no competing interests.

Figure legends (for main text figures)

Fig. 1 Changes in LSWT during 1979–2022. a Spatial distribution of trends in annual mean LSWT (°C decade^{-1}). **b** Spatial distribution of trends in summer mean LSWT (°C decade^{-1}). Note the different colour bar ranges. The *p* values of trends were calculated using a two-tailed test.

Fig. 2 HTEs in ERA5-Land during 1979–2022. a-b Temporal variations of HTE duration (days; **a**) and cumulative intensity (°C days; **b**) averaged across all studied lakes. Trends are shown in the upper left corner of each figure. **c-d** Spatial distribution of trends in HTE duration (days decade^{-1}, **c**) and trends in HTE cumulative intensity (°C days decade^{-1}, **d**). The *p* values of trends were calculated using a two-tailed test.

Fig. 3 Contribution of HTE metrics to the variation of summer mean LSWT. a The explained variance ratio of linear regression models. **b** The proportion of trends in summer mean LSWT that can be explained by HTE metrics. Note the different colour bar ranges.

Fig. 4 Contribution of HTEs to the trend in summer mean LSWT. a Probability density of trends in summer mean LSWT. The two-sided *p* value of a Kolmogorov-Smirnov test is shown. **b** Interannual variations of summer mean LSWT in CTL and CFT. **c** The contribution of HTEs to trends in summer mean LSWT. **d** The trend in summer mean LSWT differences between CTL and CFT (i.e., CTL minus CFT; °C decade^{-1}).

References

1. Coumou, D. & Rahmstorf, S. A decade of weather extremes. *Nat Clim Change* 2, 491-496 (2012).
2. Seneviratne, S. I.*, et al. Weather and climate extreme events in a changing climate* Ch. 11 (Cambridge University Press, 2021).
3. Alexander, L. V.*, et al.* Global observed changes in daily climate extremes of temperature and precipitation. *J Geophys Res* 111, D05109 (2006).
4. Mueller, B. & Seneviratne, S. I. Hot days induced by precipitation deficits at the global scale. *Proceedings of the National Academy of Sciences* 109, 12398-12403 (2012).

5. Seneviratne, S. I., *et al.* No pause in the increase of hot temperature extremes. *Nat Clim Change* 4, 161-163 (2014).
6. Witze, A. *Nature* 608, 464-465 (2022).
7. Sanderson, K. *Nature* 619, 232-233 (2023).
8. Tollefson, J. *Nature* 620, 703-704 (2023).
9. van Vliet, M. T. H., *et al.* Global river water quality under climate change and hydroclimatic extremes. *Nat Rev Earth Environ* 4, 687-702 (2023).
10. Field, C. B., *et al. Summary for Policymakers* (Cambridge University Press, 2012).
11. Callahan, C. W. & Mankin, J. S. Globally unequal effect of extreme heat on economic growth. *Sci Adv* 8, eadd3726 (2022).
12. Piao, S., *et al.* The impacts of climate change on water resources and agriculture in China. *Nature* 467, 43-51 (2010).
13. Costanza, R., *et al.* The value of the world's ecosystem services and natural capital. *Nature* 387, 253-260 (1997).
14. Sterner, R. W., *et al.* Ecosystem services of Earth's largest freshwater lakes. *Ecosyst Serv* 41, 101046 (2020).
15. O'Reilly, C. M., *et al.* Rapid and highly variable warming of lake surface waters around the globe. *Geophys Res Lett* 42, 10773-10781 (2015).
16. Woolway, R. I., *et al.* Global lake responses to climate change. *Nat Rev Earth Environ* 1, 388-403 (2020).
17. Woolway, R. I., Sharma, S. & Smol, J. P. Lakes in hot water: The impacts of a changing climate on aquatic ecosystems. *Bioscience* 72, 1050-1061 (2022).
18. Jane, S. F., *et al.* Widespread deoxygenation of temperate lakes. *Nature* 594, 66-70 (2021).
19. Søndergaard, M., Jensen, J. P. & Jeppesen, E. Role of sediment and internal loading of phosphorus in shallow lakes. *Hydrobiologia* 506-509, 135-145 (2003).
20. Till, A., *et al.* Fish die-offs are concurrent with thermal extremes in north temperate lakes. *Nat Clim Change* 9, 637-641 (2019).
21. Jankowski, T., *et al.* Consequences of the 2003 European heat wave for lake temperature profiles, thermal stability, and hypolimnetic oxygen depletion: Implications for a warmer world. *Limnol Oceanogr* 51, 815-819 (2006).
22. Bartosiewicz, M., *et al.* Heat-wave effects on oxygen, nutrients, and phytoplankton can alter global warming potential of gases emitted from a small shallow lake. *Environ Sci Technol* 50, 6267-6275 (2016).
23. Kangur, K., *et al.* Long-term effects of extreme weather events and eutrophication on the fish community of shallow Lake Peipsi (Estonia/Russia). *J Limnol* 72, 376-387 (2013).
24. Grant, L., *et al.* Attribution of global lake systems change to anthropogenic forcing. *Nat Geosci* 14, 849-854 (2021).
25. Woolway, R. I., Jennings, E. & Carrea, L. Impact of the 2018 European heatwave on lake surface water temperature. *Inland Waters* 10, 322-332 (2020).
26. Wang, W., *et al.* A record-breaking extreme heat event caused unprecedented warming of lakes in China. *Sci Bull (Beijing)* 68, 578-582 (2023).
27. Barriopedro, D., *et al.* The hot summer of 2010: Redrawing the temperature record

map of Europe. *Science* 332, 220-224 (2011).
28. Woolway, R. I.*, et al.* Lake heatwaves under climate change. *Nature* 589, 402-407 (2021).
29. Schneider, P. & Hook, S. J. Space observations of inland water bodies show rapid surface warming since 1985. *Geophys Res Lett* 37, L22405 (2010).
30. Muñoz-Sabater, J.*, et al.* ERA5-Land: A state-of-the-art global reanalysis dataset for land applications. *Earth Syst Sci Data* 13, 4349-4383 (2021).
31. Mironov, D. *Parameterization of lakes in numerical weather prediction: Description of a lake model* (Deutscher Wetterdienst, Offenbach, 2008).
32. Wang, X.*, et al.* Climate change drives rapid warming and increasing heatwaves of lakes. *Sci Bull (Beijing)* 68, 1574-1584 (2023).
33. Carrea, L.*, et al.* Lake surface water temperature [in "State of the Climate in 2022"]. *Bull Amer Meteor Soc* 104, S28-S30 (2022).
34. Winslow, L. A.*, et al.* Seasonality of change: Summer warming rates do not fully represent effects of climate change on lake temperatures. *Limnol Oceanogr* 62, 2168-2178 (2017).
35. Shabbar, A. & Bonsal, B. An assessment of changes in winter cold and warm spells over Canada. *Nat Hazards* 29, 173-188 (2003).
36. Chapman, S. C.*, et al.* Trends in winter warm spells in the central England temperature record. *J Appl Meteorol Clim* 59, 1069-1076 (2020).
37. Li, X.*, et al.* Earlier ice loss accelerates lake warming in the Northern Hemisphere. *Nat Commun* 13, 5156 (2022).
38. Arvola, L.*, et al. The impact of the changing climate on the thermal characteristics of lakes* Ch. 6 (Springer Dordrecht, 2009).
39. Rousi, E.*, et al.* Accelerated western European heatwave trends linked to more-persistent double jets over Eurasia. *Nat Commun* 13, 3851 (2022).
40. Byrne, M. P. Amplified warming of extreme temperatures over tropical land. *Nat Geosci* 14, 837-841 (2021).
41. Sun, Y.*, et al.* Rapid increase in the risk of extreme summer heat in Eastern China. *Nat Clim Change* 4, 1082-1085 (2014).
42. Thompson, V.*, et al.* The most at-risk regions in the world for high-impact heatwaves. *Nat Commun* 14, 2152 (2023).
43. Schewe, J.*, et al.* State-of-the-art global models underestimate impacts from climate extremes. *Nat Commun* 10, 1005 (2019).
44. Al-Yaari, A.*, et al.* Heatwave characteristics in the recent climate and at different global warming levels: A multimodel analysis at the global scale. *Earth's Future* 11, e2022EF003301 (2023).

Methods

Study sites

We selected 1260 lakes around the world from the HydroLAKES dataset[45] according to

the availability of satellite observations and model performance (Extended Data Fig. 1). These lakes are situated across North America (n = 489), Asia (n = 276), Europe (n = 297), South America (n = 103), Africa (n = 51), and Oceania (n = 44), covering different climate zones.

ERA5-Land

The ERA5-Land dataset provides land surface variables at hourly time intervals and a spatial resolution of 0.1° × 0.1°[30]. Although ERA5-Land is one of the most state-of-art reanalysis datasets, its spatial resolution of 0.1° is coarse for small lakes. To address this issue, we extracted data from the nearest ERA5-Land grid cell nearest to the lake centres in order to drive the lake model effectively (see Simulated LSWT). The remaining potential errors in the meteorological forcing can be compensated in the parameter-tuning procedure (see Simulated LSWT).

Observed LSWT

The European Space Agency Climate Change Initiative project (Lakes_cci) provides daily lake skin temperature at 1 km resolution[46] from 2000 to 2020. We computed zonal mean skin temperature using the lake outlines from HydroLAKES to represent the LSWT for each lake. We used Lakes_cci during 2000–2010 (2011–2020) to calibrate (validate) the model parameters in the tuning procedure (see Simulated LSWT). To minimize the uncertainties in satellite products, only satellite data with the best quality (quality flag = 5) were used in this study. The discrepancy between best-quality Lakes_cci and in-situ LSWT is very low (~ 0.1 °C)[46]. Except for Lakes_cci, multi-source satellite products and in-situ LSWT were used in this study to validate the modelled LSWT, for instance, the Global Observatory of Lake Responses to Environmental Change (GloboLakes) dataset, which also includes daily lake skin temperature

but with a coarser resolution (0.05° × 0.05°)[47] from June 1995 to 2016. We applied the same method used for Lakes_cci to process GloboLakes and used data from June 1995 to 1999 to validate the modelled daily mean LSWT.

The Global Lake Temperature Collaboration (GLTC) dataset provides summer mean in-situ LSWT and satellite-derived skin temperature for 291 lakes worldwide during 1985–2009[48]. It was used to validate the modelled summer mean LSWT. Furthermore, we collected in-situ LSWT measurements with time intervals ranging from hourly to daily from seven Chinese lakes during 1993–2022 and averaged them into daily intervals for comparisons with modelled daily mean LSWT. In-situ LSWT from GLTC and seven Chinese lakes were measured between 0 and 3 m below the surface. The characteristics, sampling depth and distribution of all the lakes with in-situ measurements (n = 29) can be found in Supplementary Table 1 and Supplementary Fig. 1.

Simulated LSWT

We used the FLake model to simulate hourly LSWT from 1979 to 2022 for all studied lakes. FLake is an approximation procedure of LSWT developed by the German Meteorological Service[31]. It solves the surface heat balance to estimate LSWT and does not explicitly formulate the heat transfer in the water column, instead adopting the self-similarity theory, in which the vertical heat distribution is represented by polynomial curves[31]. The simple model structure greatly benefits its computation efficiency[49] and allows for widespread global application[28]. However, lake characteristics are highly heterogeneous and critical in shaping lake thermal structure, implying the necessity to tune lake-specific model parameters for each site. Therefore, we used an automatic tuning procedure that calibrates FLake by minimizing root mean square

errors (RMSEs) between modelled LSWT and Lakes_cci, namely as the coupling remote sensing observations and FLake (CSFLake) approach[32]. Three model parameters were tuned, i.e., the light extinction coefficient (influences the amount of solar radiation reaching each water layer), lake ice albedo (influences the date of ice-on and ice-off), and a multiplication factor to adjust the mean lake depth (complements the potential uncertainties of average depths). Notably, many processes affecting LSWT are omitted in FLake, for instance, horizontal circulations, cold inflows from glacial meltwater, the salinity of water, etc. The assumed two-layer water column in FLake also limits its application in very shallow or deep lakes. Hence, in this study, we chose study sites considering both the availability of satellite observations and model performances, i.e., if the lake with unresolved processes cannot be well simulated by calibrating the aforementioned three model parameters, it was excluded in this research. More details about CSFLake can be found in ref. [32].

We conducted two numerical experiments, i.e., CTL and CFT. In CTL, hourly ERA5-Land was used to drive FLake and generate a realistic substitute of the real world from 1979-01-01 00:00 (UTC) to 2022-12-31 23:00. The meteorological forcing required to run FLake (as described in ERA5-Land) includes 2-m air temperature (K), 2-m specific humidity (kg kg^{-1}), 10-m wind speed (m s^{-1}), surface pressure (Pa), surface solar radiation downwards (W m^{-2}), and surface thermal radiation downwards (W m^{-2}). Furthermore, it is essential to ensure that appropriate initial values are prepared for the model integration process. We assumed that each of the studied lakes were fully mixed at the start of our simulations. The temperature profiles for both the water column and sediment were determined by selecting the higher value between the annual mean air temperature in 1979 of ERA5-Land and the water temperature associated

with maximum density. As observations during the initial starting point for all lakes are unavailable, we repeated the 1979–2022 simulation twice to provide the model with a spin-up period of 44 years to reach physically consistent states from roughly estimated initial states – this procedure is often referred to as a "perpetual year solution". As suggested by the model's official site, we turned off the snow module that is under development.

In CFT, the model parameters were the same as in CTL, except that HTEs were removed from the forcing data. When calculating the contribution value for a specific region or all study sites, we followed three steps: (1) we computed the LSWT averaged across all the studied lakes in the desired region. These results are aggregations of LSWT from multiple lakes, denoted as $\mathrm{aggLSWT}_{\mathrm{CTL}}$ and $\mathrm{aggLSWT}_{\mathrm{CFT}}$ for CTL and CFT, respectively; (2) we computed the trends of $\mathrm{aggLSWT}_{\mathrm{CTL}}$ and $\mathrm{aggLSWT}_{\mathrm{CFT}}$, which are denoted as $\mathrm{aggTrend}_{\mathrm{CTL}}$ and $\mathrm{aggTrend}_{\mathrm{CFT}}$; (3) we computed the contribution value according to the following equation:

$$\frac{\mathrm{aggTrend}_{\mathrm{CTL}} - \mathrm{aggTrend}_{\mathrm{CFT}}}{\mathrm{aggTrend}_{\mathrm{CTL}}} \times 100\% \quad (2)$$

Time series analysis

The original simulation results from CTL and CFT were at hourly time intervals. We first removed LSWTs ≤ 1 °C[50] to exclude ice-cover periods. Then we calculated daily, summer, and annual mean LSWT time series for comparisons and analyses. Theil-Sen estimator was used to compute long-term trends.

Detection of LHWs

We calculated LHWs following the definition in ref. [28], but without sampling and smoothing windows to avoid summer statistics being affected by LSWT in other months. If the time gap between two LHWs is less than two days, they are considered as one event that is

interrupted and combined into one[28]. We selected two metrics to describe the length and severity of LHWs: the duration (days) and cumulative intensity (°C days). The cumulative intensity is defined as

$$\sum_{i=0}^{n} [T(i) - T_m(i)] \quad (3)$$

where i refers to each day of HTEs in one year, T refers to air temperature on day i, and T_m refers to the climatological mean (relative to 1979–2022) air temperature on day i. We computed the total duration and mean cumulative intensity for LHWs in each year and summer to represent the interannual variation, and only summer statistics were used in the contribution analysis.

Validation of simulated LSWT and LHWs

The tuning procedure CSFLake substantially improves model performance (Extended Data Fig. 2), narrowing correlation coefficients and RMSEs to a range of 0.89–0.99 [0.73, 0.99] and 0.9–1.8 [0.6, 2.0] °C, while elevating the correlation coefficient averaged over all lakes to 0.96 and lowering the RMSE to 1.4 °C. During the summer months, the simulations maintain a high degree of accuracy, despite slight decreases in correlation coefficients attributed to the narrower range of LSWT variation. On average, the correlation coefficient and RMSE are 0.89 (0.70) and 1.3 °C (1.3 °C) across the studied lakes in the Northern Hemisphere (Southern Hemisphere). To further validate the reliability of the simulation results, we conducted comparative assessments against other satellite products and in-situ measurements from 29 lakes worldwide, achieving satisfactory agreements (Extended Data Fig. 3).

We used satellite data as a reference to determine whether the model can simulate lake heatwaves. Specifically, we detected lake heatwaves from Lakes_cci and simulated LSWT from

2000 to 2020 and compared their LHW metrics. We created data gaps in the modelled daily mean LSWT the same as Lakes_cci to ensure that LHWs detected from model results and satellite data can be directly compared. However, these data gaps make it difficult to satisfy the "prolonged" criteria in the definition of LHWs. To address this issue, we used a lower threshold of LHWs, which is used for the comparison only, i.e., daily lake temperature exceeds the 60th percentile of the 2000–2020 distribution for at least three consecutive days. By detecting more LHWs, we can include data from a wider range of lakes in our comparisons.

Lakes_cci and CTL have good agreements for both LHW duration and cumulative intensity (Extended Data Fig. 6). From 2000 to 2020, the mean absolute bias of LHW duration and cumulative intensity were 0.7 days and 0.5 °C days. Mean LHW cumulative intensity and duration derived from simulation results and satellite observations exhibit correlation coefficients of 0.91 and 0.96, with RMSEs of 0.8 °C days and 1.2 days.

Data availability

ERA5-Land reanalysis is available to download from https://cds.climate.copernicus.eu/cdsapp#!/dataset/reanalysis-era5-land?tab=overview. Lakes_cci is available to download from https://data.ceda.ac.uk/neodc/esacci/lakes/data/lake_products/L3S/v2.0. GloboLakes is available to download from https://catalogue.ceda.ac.uk/uuid/76a29c5b55204b66a40308fc2ba9cdb3. GLTC is available to download from https://doi.org/10.6073/pasta/89bacfc9dfcabce545ae11b353a8e5fd. Daily LSWT in the CTL and CFT experiments and a table of lake characteristics are provided at

https://doi.org/10.11888/Terre.tpdc.301309[51]. Data used to create figures are available from https://doi.org/10.5281/zenodo.13189352[52].

Code availability

The source code of the FLake model can be found at http://www.flake.igb-berlin.de. Codes used to generate figures in the manuscript are available at https://zenodo.org/records/13189352[51].

Methods references

45. Messager, M. L., *et al.* Estimating the volume and age of water stored in global lakes using a geo-statistical approach. *Nat Commun* 7, 13603 (2016).
46. Carrea, L., *et al.* Satellite-derived multivariate world-wide lake physical variable timeseries for climate studies. *Sci Data* 10, 30 (2023).
47. Carrea, L. & Merchant, C. J. GloboLakes: Lake surface water temperature (LSWT) v4.0 (1995–2016). Centre for Environmental Data Analysis http://dx.doi.org/10.5285/76a29c5b55204b66a40308fc2ba9cdb3 (2019).
48. Sharma, S., *et al.* A global database of lake surface temperatures collected by in situ and satellite methods from 1985-2009. *Sci Data* 2, 1-19 (2015).
49. Thiery, W. I. M., *et al.* LakeMIP Kivu: evaluating the representation of a large, deep tropical lake by a set of one-dimensional lake models. *Tellus A: Dyn Meteorol* 66, 21390 (2014).
50. Layden, A., MacCallum, S. N. & Merchant, C. J. Determining lake surface water temperatures worldwide using a tuned one-dimensional lake model. *Geosci Model Dev* 9, 2167-2189 (2016).
51. Shi, K., Wang, X. Daily lake surface water temperature for 1260 lakes worldwide (1979-2022). National Tibetan Plateau / Third Pole Environment Data Center. https://doi.org/10.11888/Terre.tpdc.301309 (2024).
52. Wang X. wangxiwen2021/HotTemperatureExtremes: v1.0 (v1.0). https://doi.org/10.5281/zenodo.13189352 (2024).

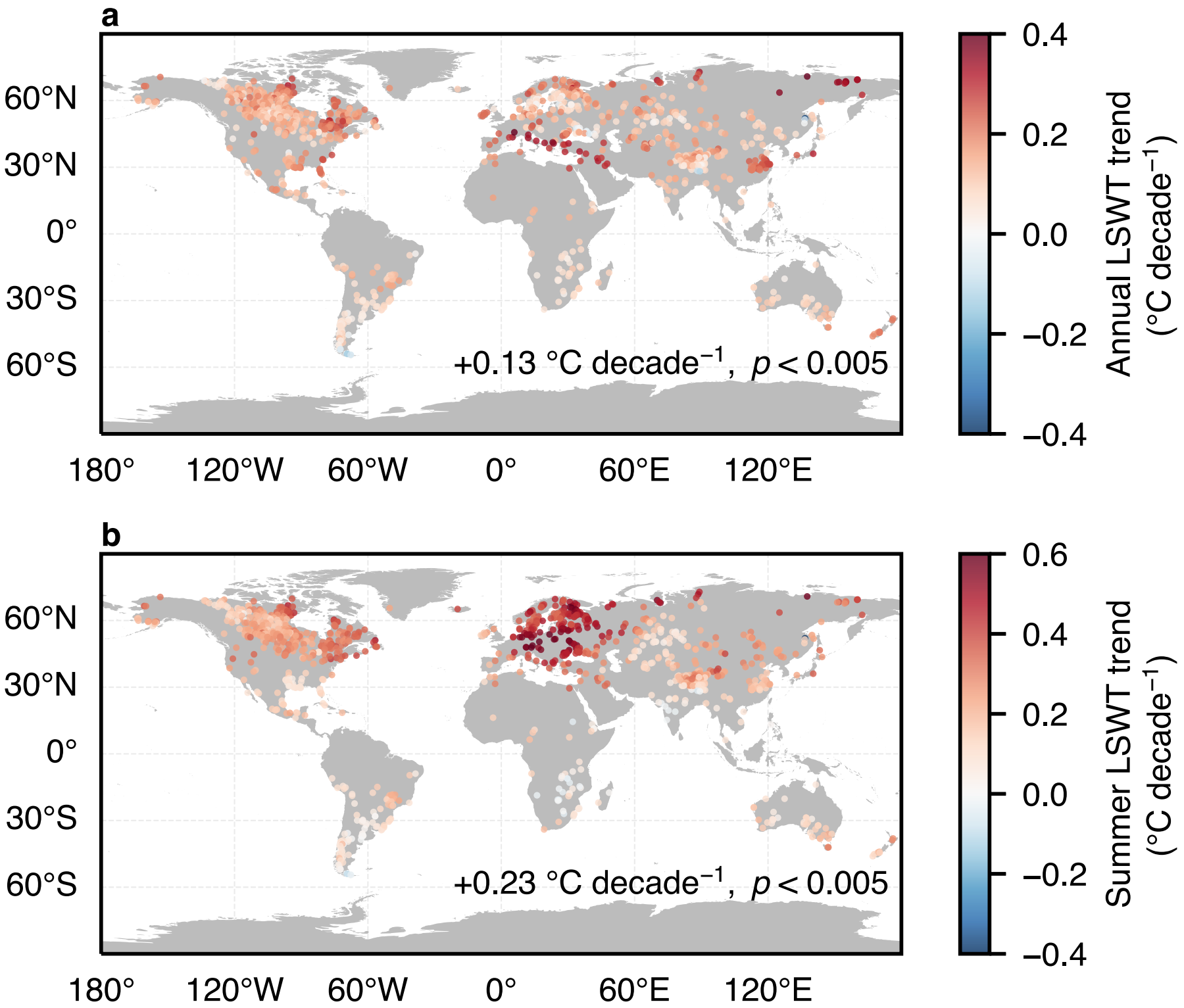
a
60°N
30°N
0°
30°S
60°S
+0.13 °C decade^{-1}, $p < 0.005$
180°
120°W
60°W
0°
60°E
120°E
0.4
0.2
0.0
−0.2
−0.4
Annual LSWT trend
(°C decade^{-1})
b
60°N
30°N
0°
30°S
60°S
+0.23 °C decade^{-1}, $p < 0.005$
180°
120°W
60°W
0°
60°E
120°E
0.6
0.4
0.2
0.0
−0.2
−0.4
Summer LSWT trend
(°C decade^{-1})

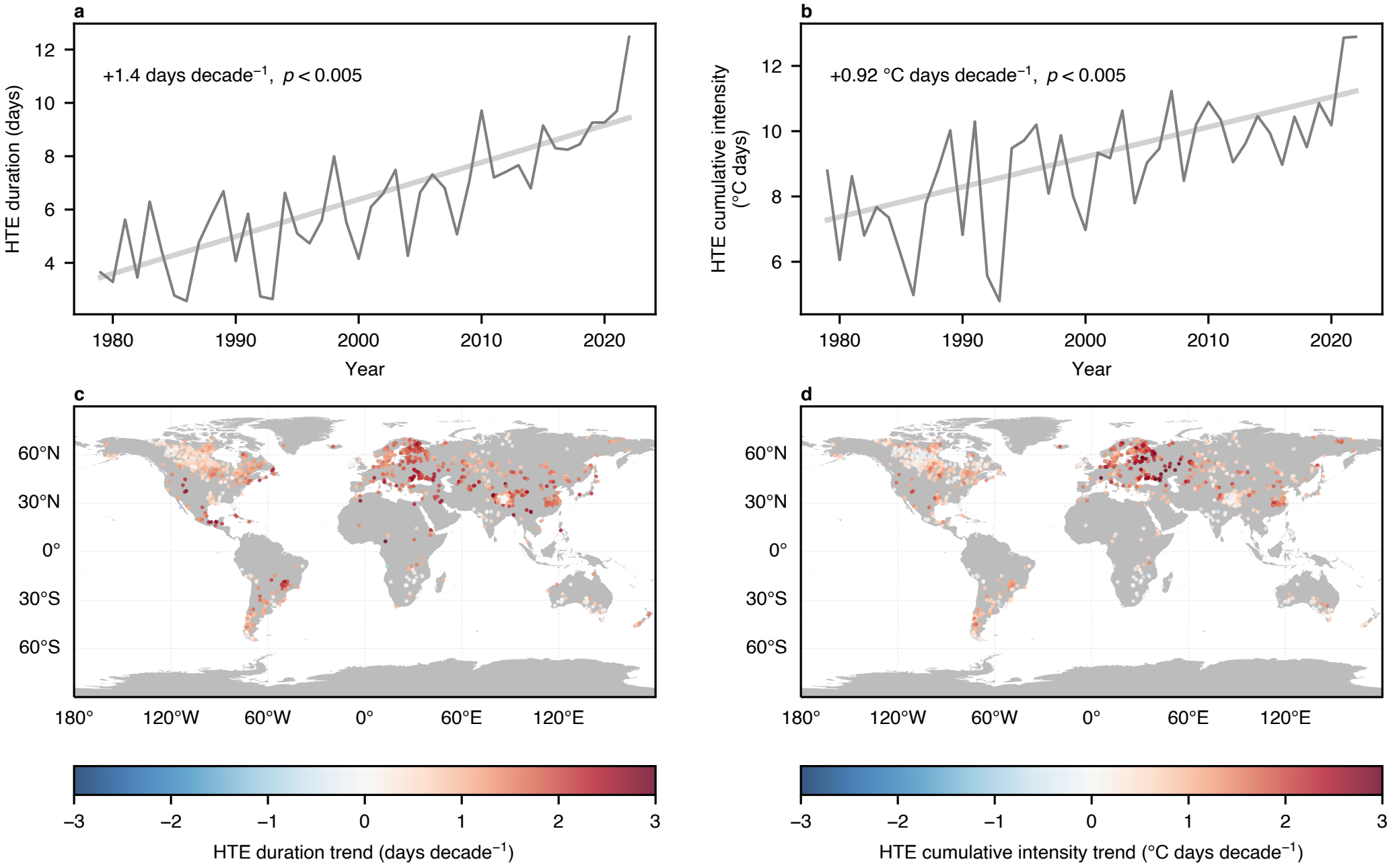
a
+1.4 days decade^{-1}, $p < 0.005$
HTE duration (days)
Year
b
+0.92 °C days decade^{-1}, $p < 0.005$
HTE cumulative intensity (°C days)
Year
c
d
60°N
30°N
0°
30°S
60°S
180°
120°W
60°W
0°
60°E
120°E
HTE duration trend (days decade^{-1})
HTE cumulative intensity trend (°C days decade^{-1})

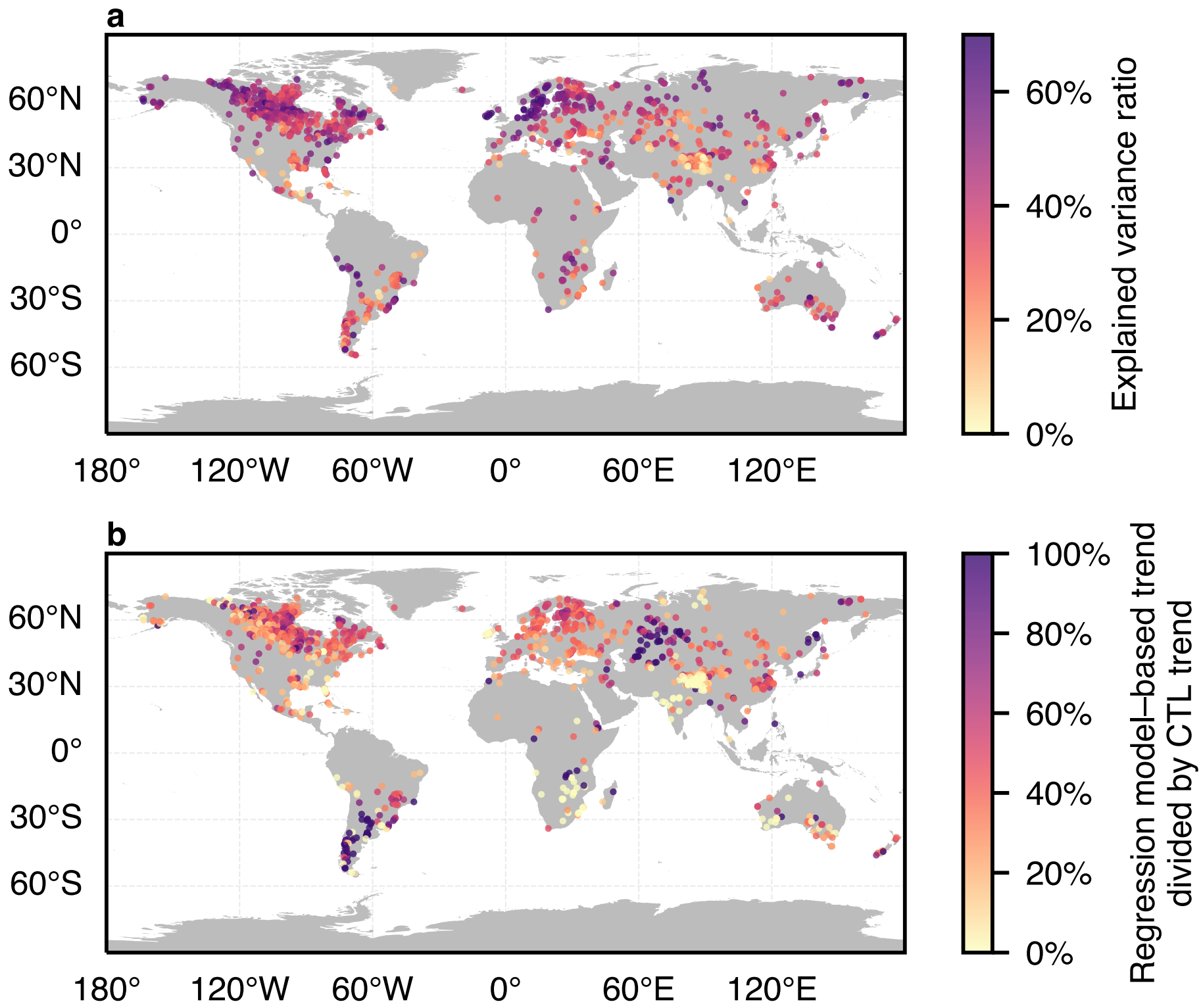
a
60°N
30°N
0°
30°S
60°S
180°
120°W
60°W
0°
60°E
120°E
60%
40%
20%
0%
Explained variance ratio
b
60°N
30°N
0°
30°S
60°S
180°
120°W
60°W
0°
60°E
120°E
100%
80%
60%
40%
20%
0%
Regression model–based trend
divided by CTL trend

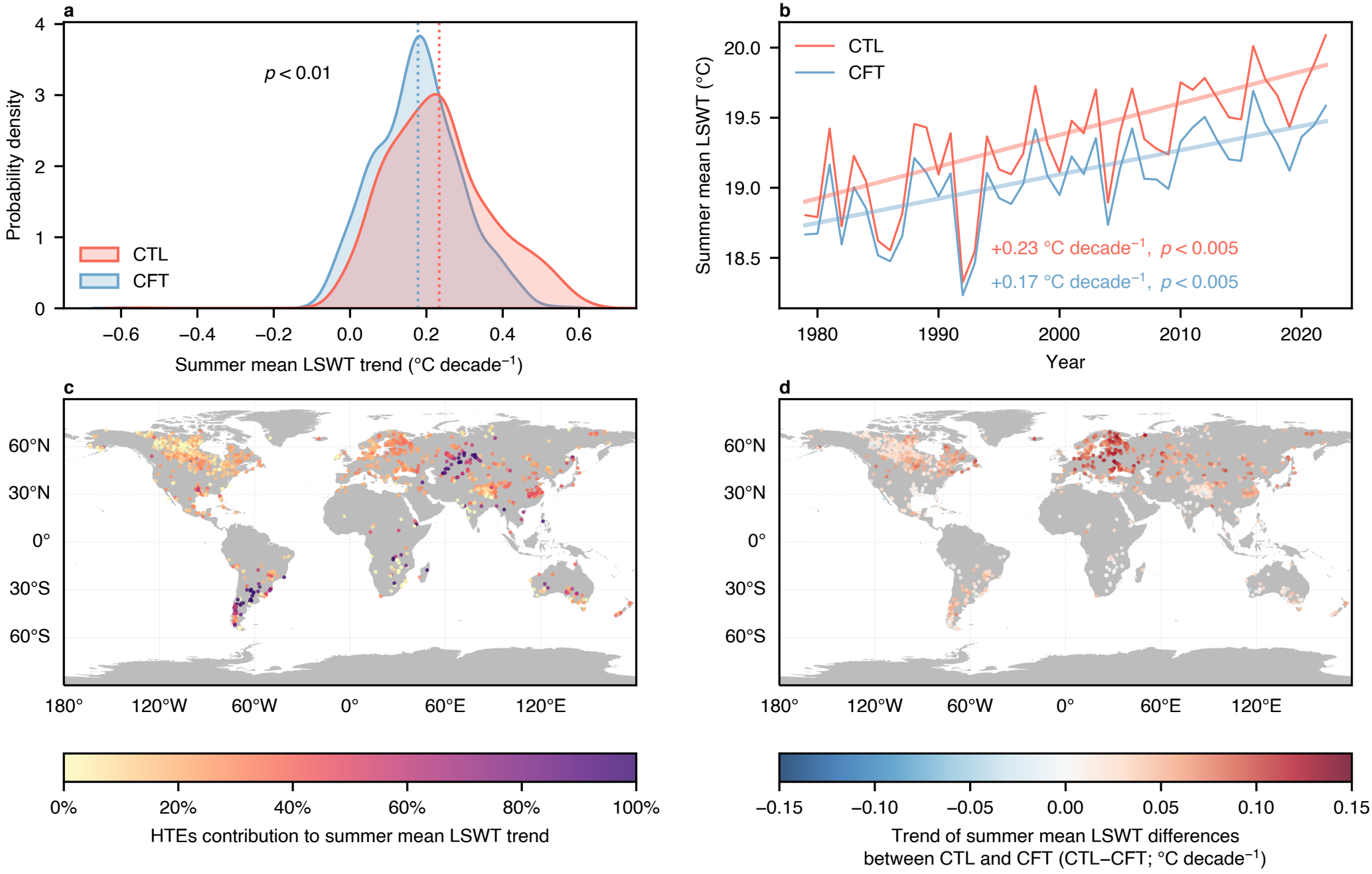
a
Probability density
p < 0.01
CTL
CFT
Summer mean LSWT trend (°C decade⁻¹)
b
Summer mean LSWT (°C)
CTL
CFT
+0.23 °C decade⁻¹, p < 0.005
+0.17 °C decade⁻¹, p < 0.005
Year
c
d
60°N
30°N
0°
30°S
60°S
180°
120°W
60°W
0°
60°E
120°E
0%
20%
40%
60%
80%
100%
HTEs contribution to summer mean LSWT trend
–0.15
–0.10
–0.05
0.00
0.05
0.10
0.15
Trend of summer mean LSWT differences
between CTL and CFT (CTL–CFT; °C decade⁻¹)

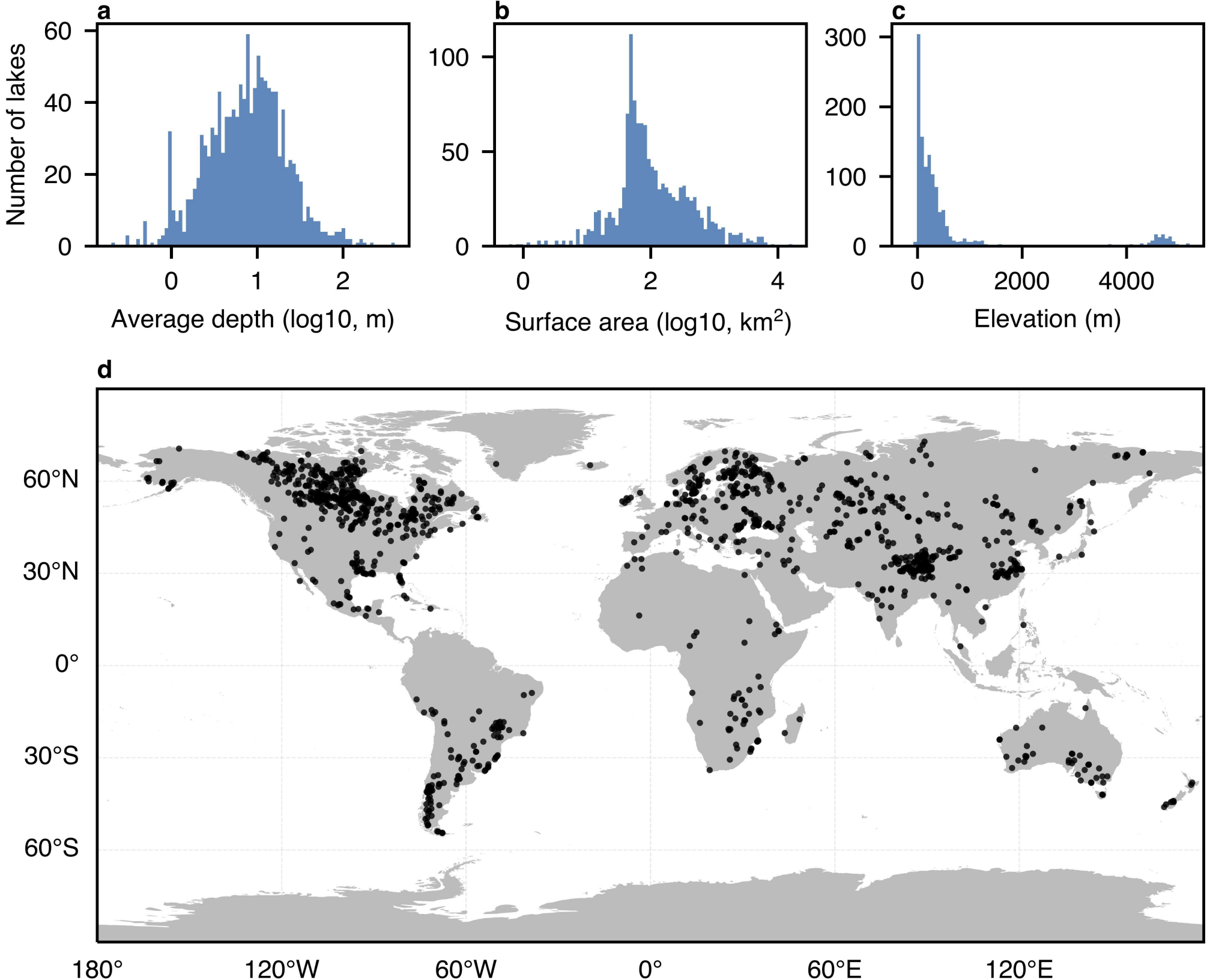
a
b
c
d
Number of lakes
60
40
20
0
0
1
2
Average depth (log10, m)
100
50
0
0
2
4
Surface area (log10, km^2)
300
200
100
0
0
2000
4000
Elevation (m)
60°N
30°N
0°
30°S
60°S
180°
120°W
60°W
0°
60°E
120°E

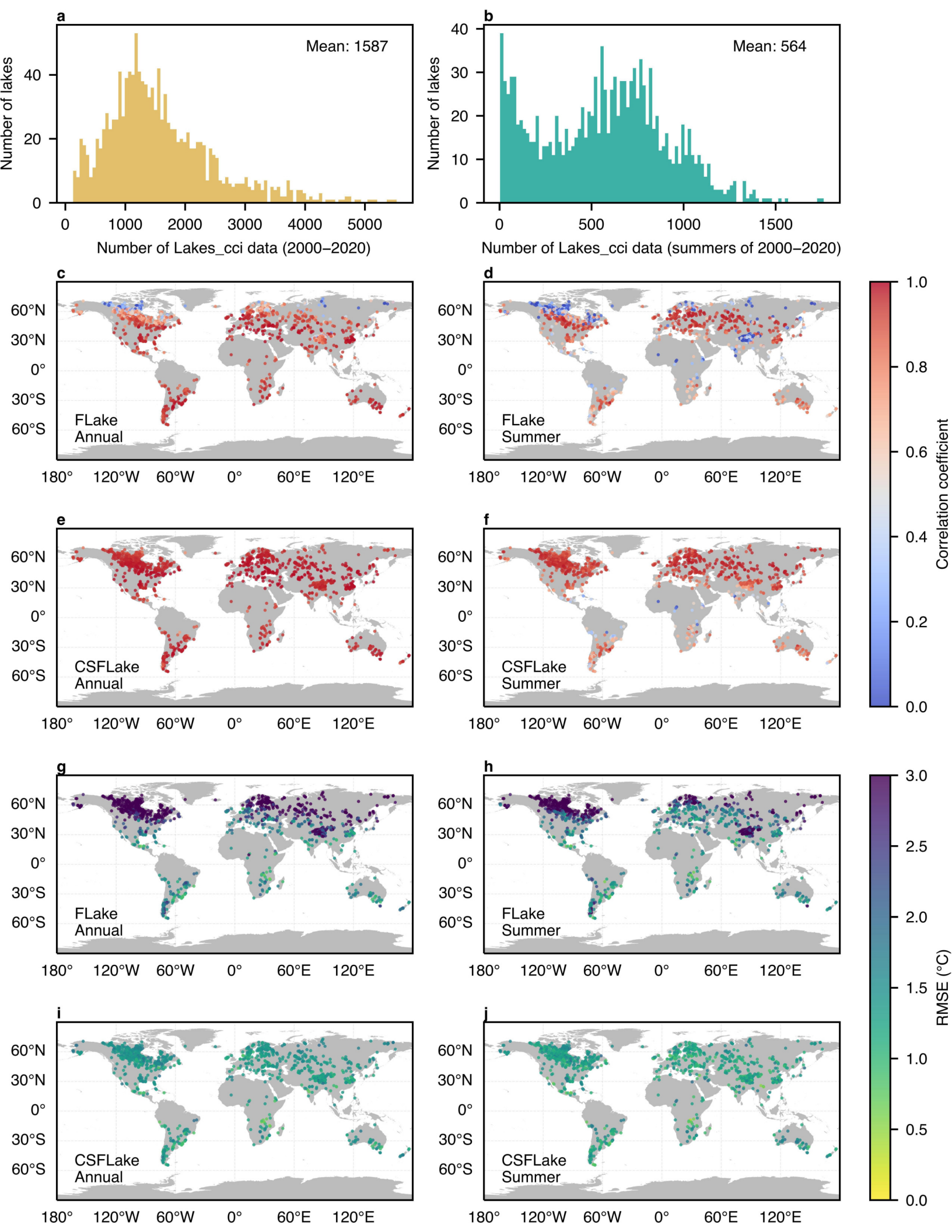
a
Mean: 1587
Number of lakes
Number of Lakes_cci data (2000–2020)
b
Mean: 564
Number of lakes
Number of Lakes_cci data (summers of 2000–2020)
c
FLake
Annual
d
FLake
Summer
e
CSFLake
Annual
f
CSFLake
Summer
g
FLake
Annual
h
FLake
Summer
i
CSFLake
Annual
j
CSFLake
Summer
60°N
30°N
0°
30°S
60°S
180°
120°W
60°W
0°
60°E
120°E
Correlation coefficient
RMSE (°C)

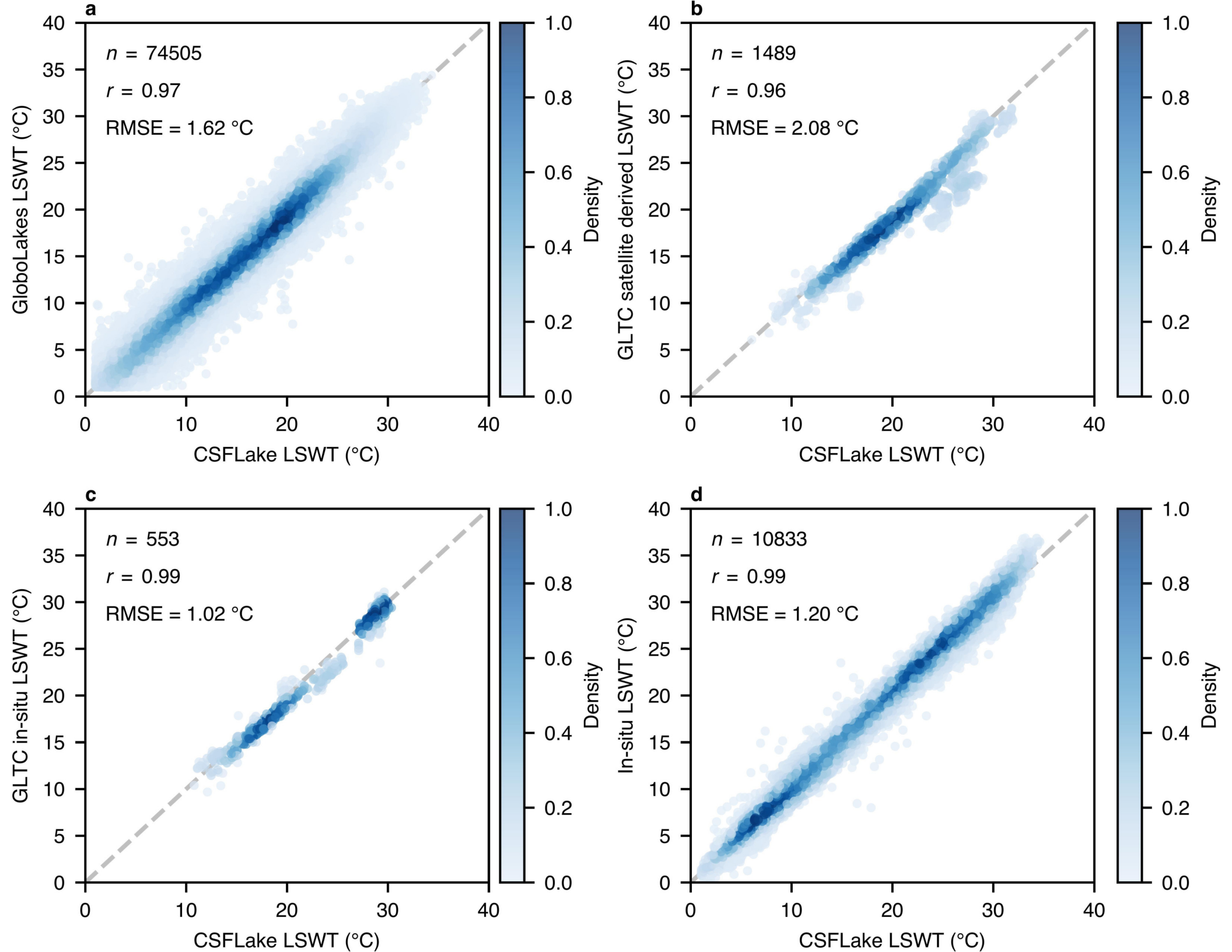
a
n = 74505
r = 0.97
RMSE = 1.62 °C
GloboLakes LSWT (°C)
CSFLake LSWT (°C)
Density
b
n = 1489
r = 0.96
RMSE = 2.08 °C
GLTC satellite derived LSWT (°C)
CSFLake LSWT (°C)
Density
c
n = 553
r = 0.99
RMSE = 1.02 °C
GLTC in-situ LSWT (°C)
CSFLake LSWT (°C)
Density
d
n = 10833
r = 0.99
RMSE = 1.20 °C
In-situ LSWT (°C)
CSFLake LSWT (°C)
Density

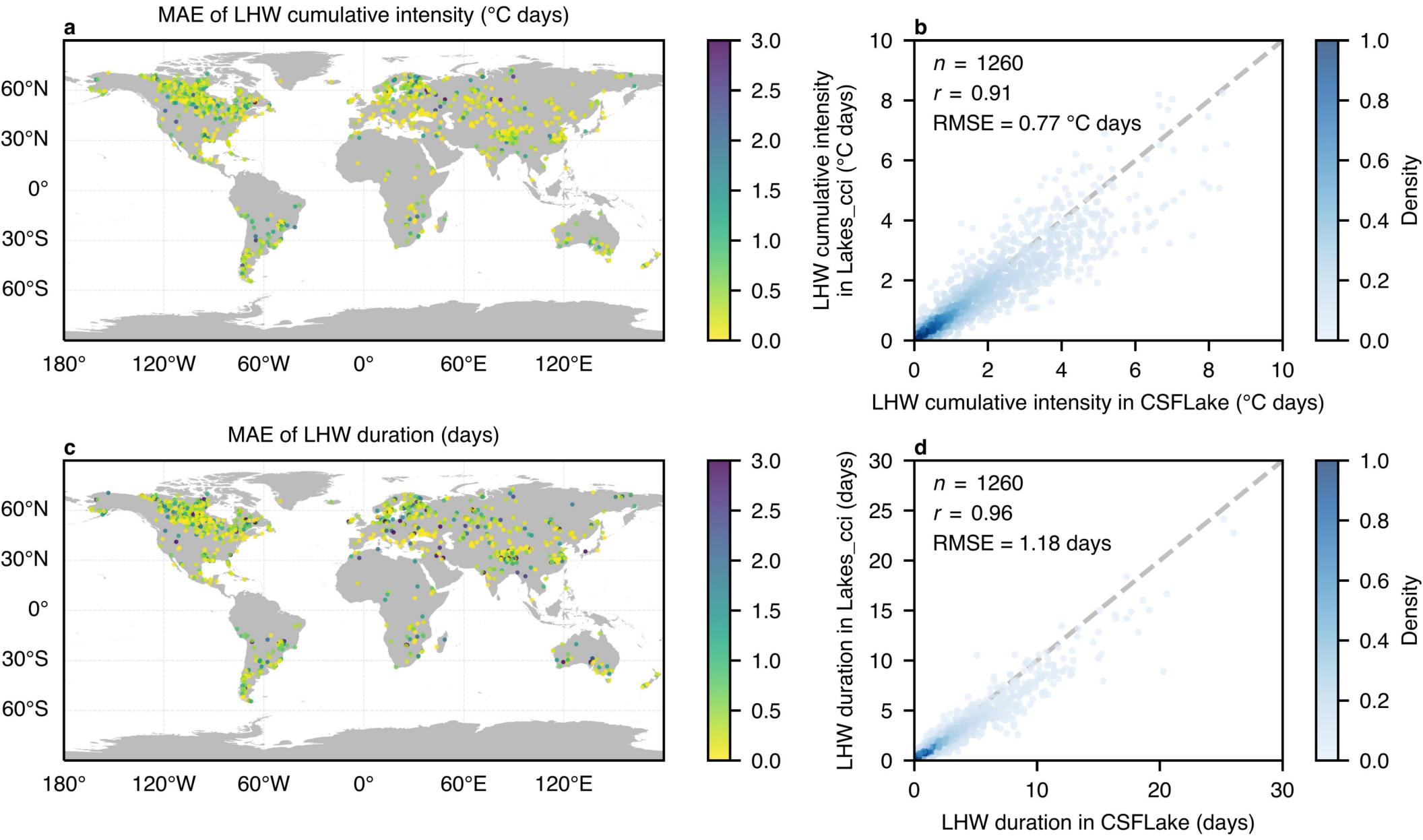
a
MAE of LHW cumulative intensity (°C days)
60°N
30°N
0°
30°S
60°S
180°
120°W
60°W
0°
60°E
120°E
3.0
2.5
2.0
1.5
1.0
0.5
0.0
b
n = 1260
r = 0.91
RMSE = 0.77 °C days
LHW cumulative intensity in Lakes_cci (°C days)
LHW cumulative intensity in CSFLake (°C days)
Density
c
MAE of LHW duration (days)
d
n = 1260
r = 0.96
RMSE = 1.18 days
LHW duration in Lakes_cci (days)
LHW duration in CSFLake (days)

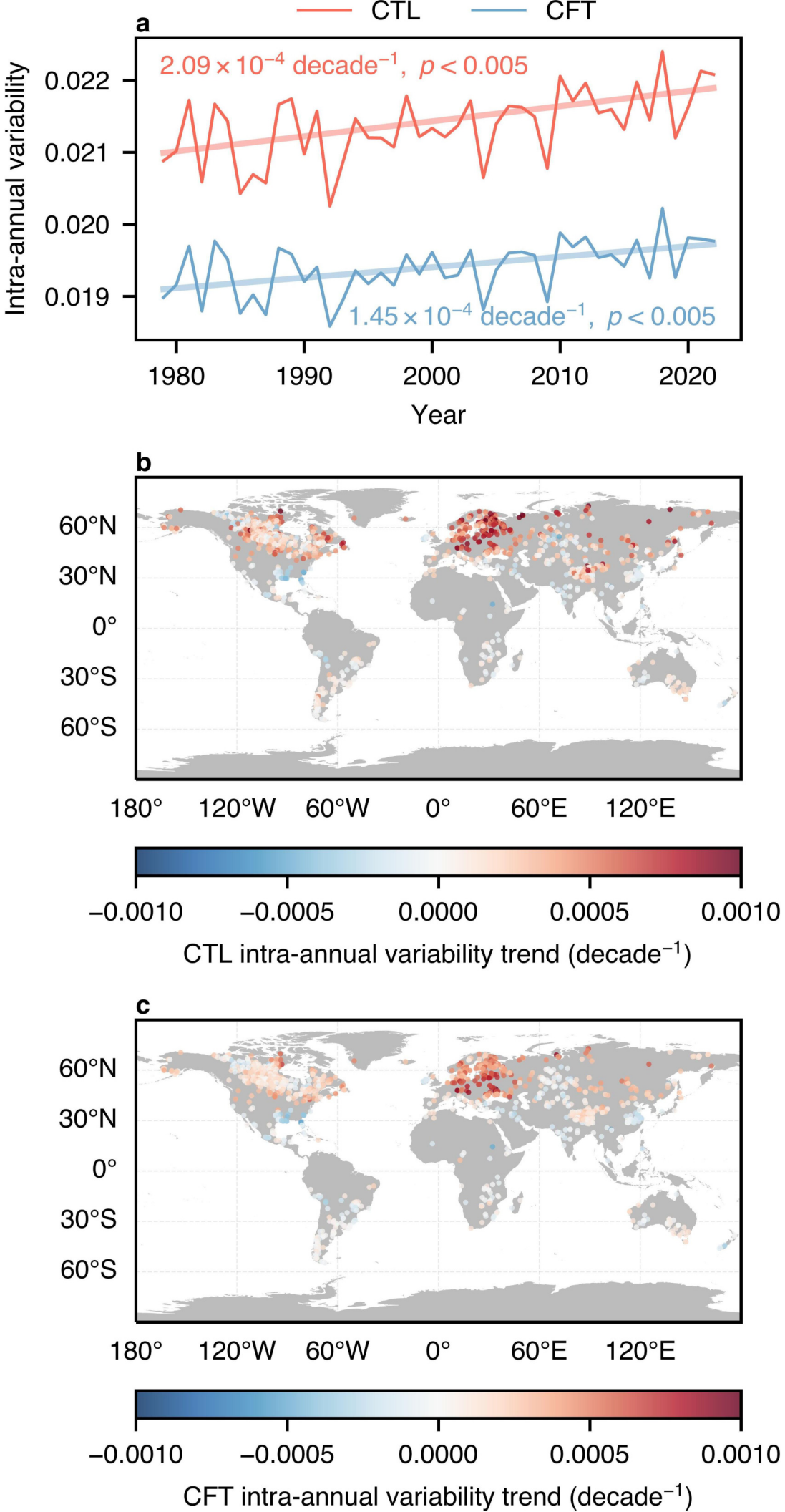
a
CTL
CFT
Intra-annual variability
0.022
0.021
0.020
0.019
2.09×10^{-4} decade^{-1}, $p < 0.005$
1.45×10^{-4} decade^{-1}, $p < 0.005$
1980
1990
2000
2010
2020
Year
b
60°N
30°N
0°
30°S
60°S
180°
120°W
60°W
0°
60°E
120°E
−0.0010
−0.0005
0.0000
0.0005
0.0010
CTL intra-annual variability trend (decade^{-1})
c
60°N
30°N
0°
30°S
60°S
180°
120°W
60°W
0°
60°E
120°E
−0.0010
−0.0005
0.0000
0.0005
0.0010
CFT intra-annual variability trend (decade^{-1})

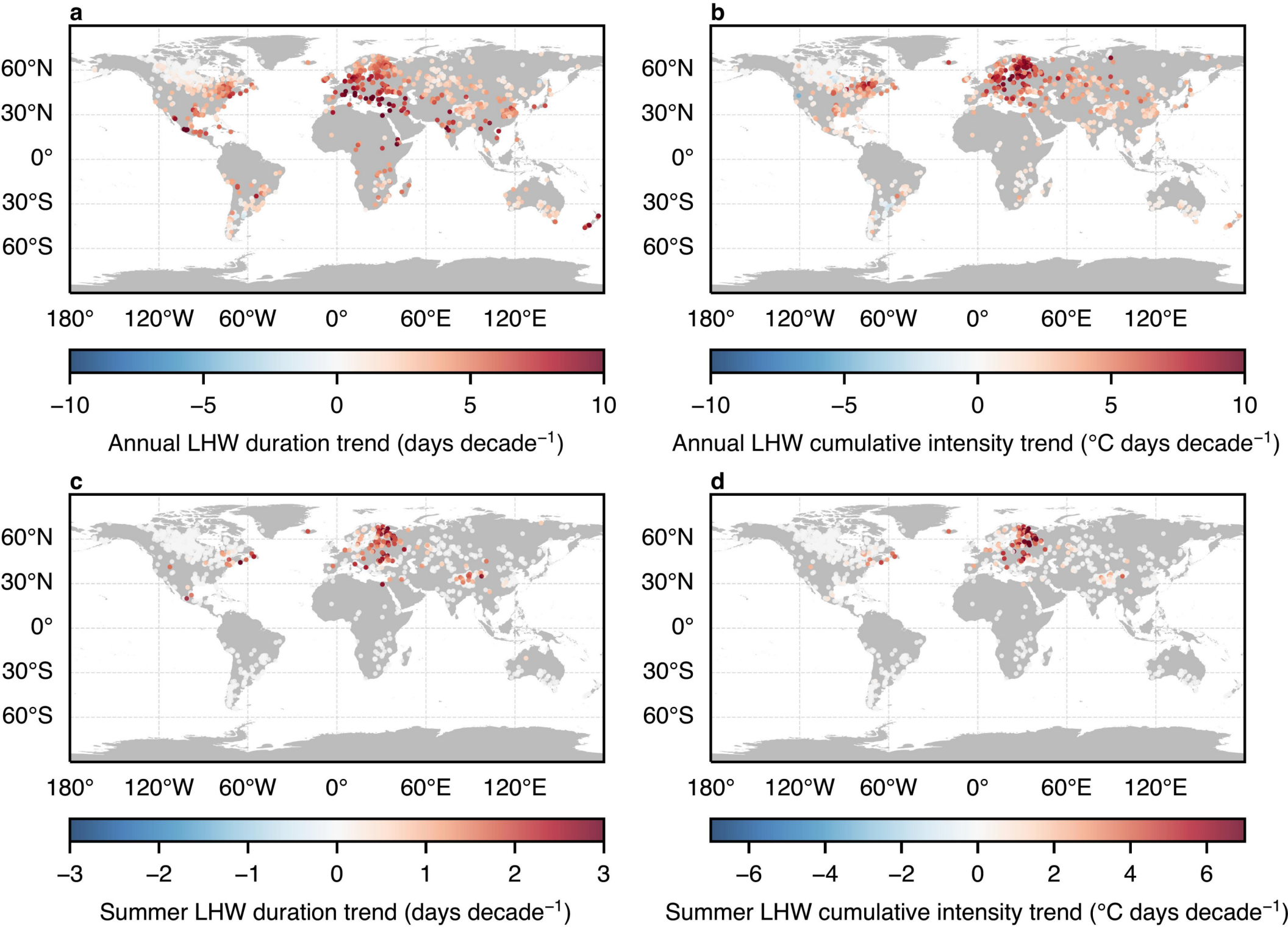
a
60°N
30°N
0°
30°S
60°S
180°
120°W
60°W
0°
60°E
120°E
−10
−5
0
5
10
Annual LHW duration trend (days decade−1)
b
60°N
30°N
0°
30°S
60°S
180°
120°W
60°W
0°
60°E
120°E
−10
−5
0
5
10
Annual LHW cumulative intensity trend (°C days decade−1)
c
60°N
30°N
0°
30°S
60°S
180°
120°W
60°W
0°
60°E
120°E
−3
−2
−1
0
1
2
3
Summer LHW duration trend (days decade−1)
d
60°N
30°N
0°
30°S
60°S
180°
120°W
60°W
0°
60°E
120°E
−6
−4
−2
0
2
4
6
Summer LHW cumulative intensity trend (°C days decade−1)

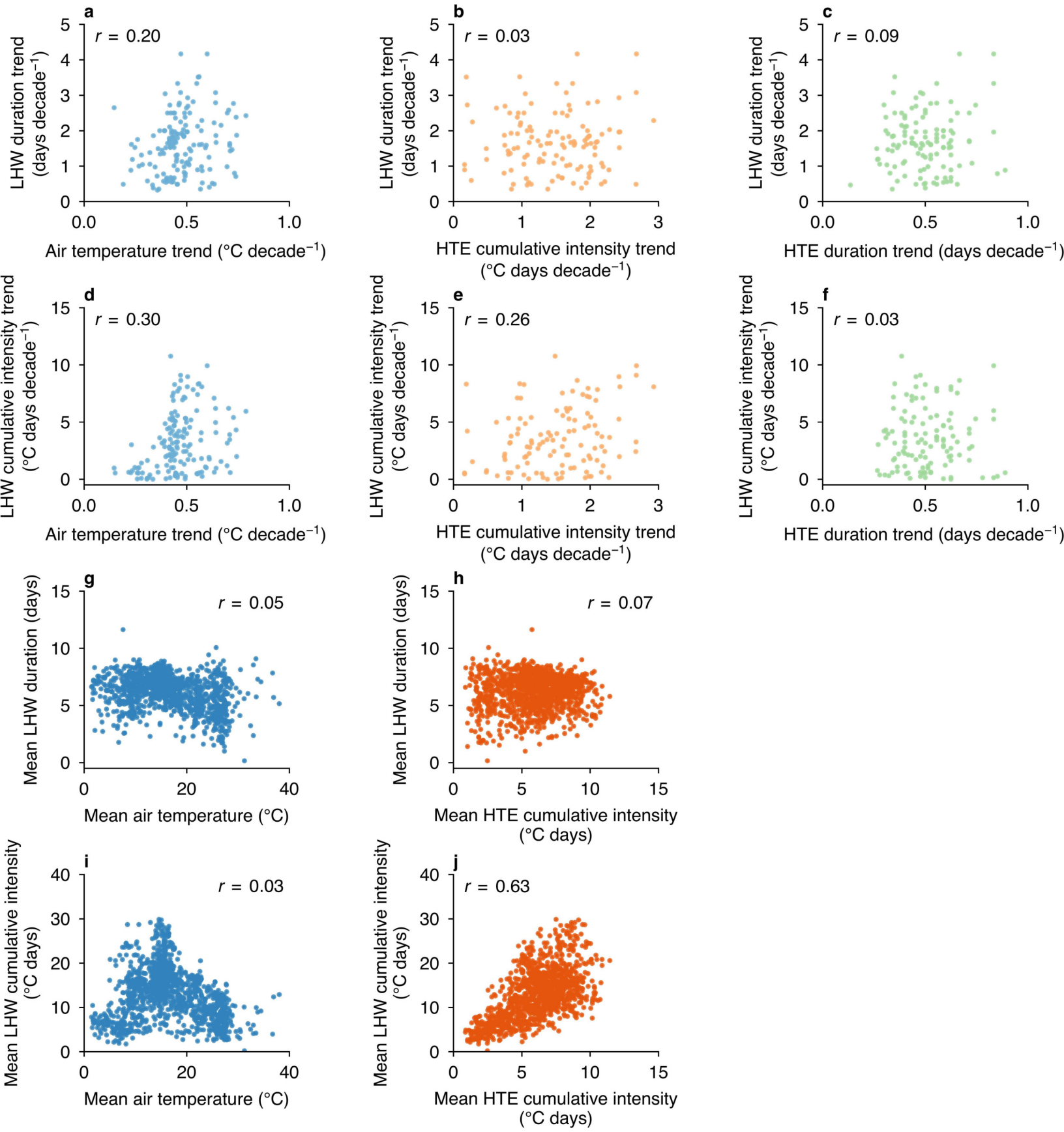
a
r = 0.20
LHW duration trend (days decade−1)
Air temperature trend (°C decade−1)
b
r = 0.03
LHW duration trend (days decade−1)
HTE cumulative intensity trend (°C days decade−1)
c
r = 0.09
LHW duration trend (days decade−1)
HTE duration trend (days decade−1)
d
r = 0.30
LHW cumulative intensity trend (°C days decade−1)
Air temperature trend (°C decade−1)
e
r = 0.26
LHW cumulative intensity trend (°C days decade−1)
HTE cumulative intensity trend (°C days decade−1)
f
r = 0.03
LHW cumulative intensity trend (°C days decade−1)
HTE duration trend (days decade−1)
g
r = 0.05
Mean LHW duration (days)
Mean air temperature (°C)
h
r = 0.07
Mean LHW duration (days)
Mean HTE cumulative intensity (°C days)
i
r = 0.03
Mean LHW cumulative intensity (°C days)
Mean air temperature (°C)
j
r = 0.63
Mean LHW cumulative intensity (°C days)
Mean HTE cumulative intensity (°C days)

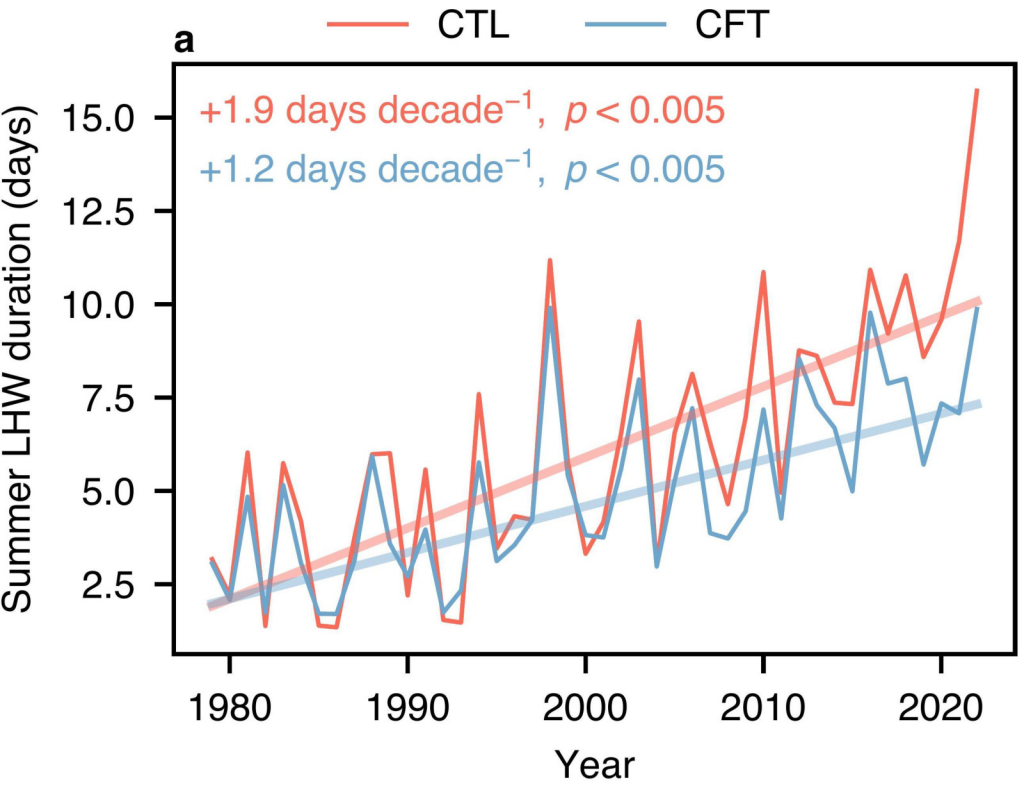
a
CTL
CFT
+1.9 days decade^{-1}, $p < 0.005$
+1.2 days decade^{-1}, $p < 0.005$
Summer LHW duration (days)
15.0
12.5
10.0
7.5
5.0
2.5
1980
1990
2000
2010
2020
Year

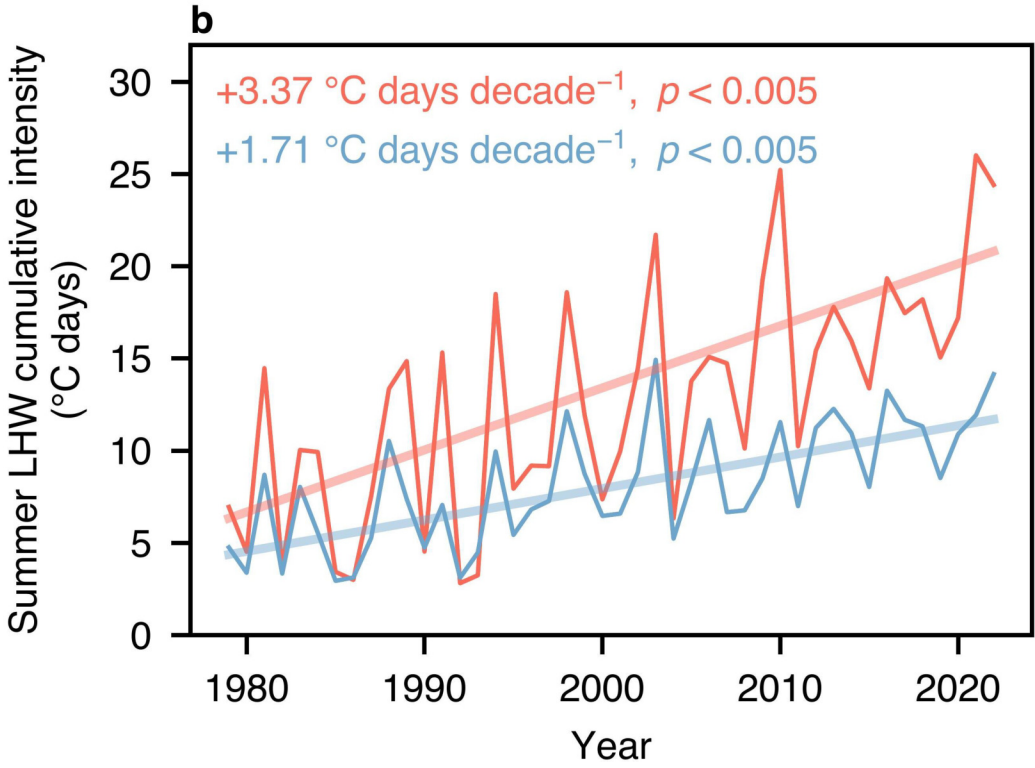
b
+3.37 °C days decade^{-1}, $p < 0.005$
+1.71 °C days decade^{-1}, $p < 0.005$
Summer LHW cumulative intensity (°C days)
30
25
20
15
10
5
0
1980
1990
2000
2010
2020
Year